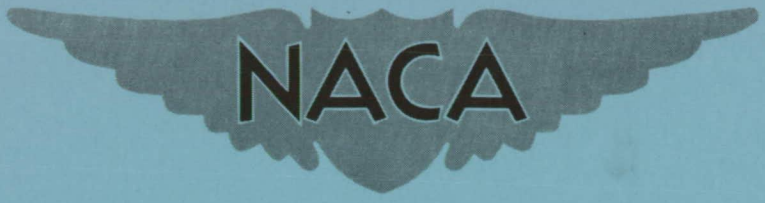

RESEARCH MEMORANDUM

THE STATIC AND DYNAMIC LONGITUDINAL STABILITY CHARACTERISTICS OF SOME SUPERSONIC AIRCRAFT CONFIGURATIONS

By Jesse L. Mitchell

Langley Aeronautical Laboratory
Langley Field, Va.

NATIONAL ADVISORY COMMITTEE
FOR AERONAUTICS

WASHINGTON

January 29, 1952
Declassified July 17, 1958

NATIONAL ADVISORY COMMITTEE FOR AERONAUTICS

RESEARCH MEMORANDUM

THE STATIC AND DYNAMIC LONGITUDINAL STABILITY CHARACTERISTICS OF SOME SUPERSONIC AIRCRAFT CONFIGURATIONS

By Jesse L. Mitchell

The purpose of this paper is to discuss some longitudinal stability characteristics of supersonic aircraft configurations. The discussion is presented under two general headings: static longitudinal stability and dynamic longitudinal stability. Some information on the variation of pitching-moment coefficient with angle of attack as influenced by the vertical location of the horizontal tail is presented in the section on static stability. The static-stability variation with Mach number and its effect on maneuverability and trim is discussed for several typical configurations on which data are available. In the dynamic stability section the short-period longitudinal oscillation is the subject of discussion. Some data on the damping-in-pitch derivatives of tailless aircraft are presented and the period and damping characteristics of some supersonic aircraft configurations are discussed.

Static Longitudinal Stability

The flow characteristics behind low-aspect-ratio wings indicate that, for a configuration having a low-aspect-ratio delta or swept wing and a horizontal tail back of the wing, the vertical location of the horizontal tail greatly influences the variation of pitching-moment coefficient with angle of attack.

The variation of pitching-moment coefficient C_m with angle of attack α for a configuration consisting of an aspect-ratio-2.0 delta wing having a horizontal tail mounted behind, either in the plane of the wing extended or at a point 0.25 semispan above the wing, is shown in figure 1. These data were obtained from Ames transonic-bump tests (reference 1) and are shown for Mach numbers of 0.40, 0.90, and 1.10. Note that at all these Mach numbers the configuration with the low horizontal tail has the more nearly linear variation of pitching moment with angle of attack. References 2 and 3 present other data which substantiate the above results.

Since the flow field characteristics behind plain, sweptback, low-aspect-ratio wings are similar to those behind delta wings, it is to be expected that a similar effect of tail height on the variation of C_m with α will exist for sweptback wing configurations. This result is confirmed at subsonic speeds (M = 0.17) and low Reynolds number (0.9×10^6) by the results presented in figure 2. These data of C_m as a function of α were obtained from tests in the Langley stability tunnel (reference 4) on an aspect-ratio-4.0, 45° sweptback wing configuration with a horizontal tail located behind either in the plane of the wing extended or at a position 0.29 semispan above the wing plane. The model with the tail in the low position also has a more nearly linear variation of C_m with α. Additional data on tail-height effect on stability at low speeds are given in references 5 and 6. No comparable data were available at higher Mach numbers. In figure 3, however, are presented some results on lift and pitching-moment variation with angle of attack at a Mach number of 0.93 for a configuration having an aspect-ratio-4.0, 45° sweptback wing and a horizontal tail mounted 0.50 semispan above the wing. The solid curves are actual test results of the complete configuration as obtained from rocket-model tests. The short-dash and long-dash curves were computed from wing-fuselage moment and lift, and downwash data from the indicated sources (references 7 and 8). The results indicate that, at least for this wing, Reynolds number effects are small.

In order to define what is meant by a high or low horizontal tail, figure 4 has been prepared. Tail positions have been plotted with reference to their distance behind and above the trailing edge of the wing mean aerodynamic chord. These tail positions have been classified as to the characteristics of the downwash at these positions. The solid points indicate a downwash variation with angle of attack in which $d\epsilon/d\alpha$ increases with increasing angle of attack; the half-solid points indicate essentially a linear variation of downwash with angle of attack; and the open points indicate a downwash variation with angle of attack in which $d\epsilon/d\alpha$ decreases with increasing angle of attack. The data were average downwash behind some ten different swept and delta wings. The range of aspect ratio, sweep, Mach number, tail span, and Reynolds number covered by the data are indicated in the figure. See references 1 to 3, 6, and 9 to 12.

All the open or half-open points fall below a line which makes an angle of about 10° from the origin. It can be expected therefore that, for swept or delta wing configurations, horizontal-tail locations on or below the 10° line shown are most likely to result in linear or more nearly linear variation of pitching moment with angle of attack.

The preceding discussion of tail height has been for delta or sweptback wing configurations. Figure 5 presents pitching-moment coefficient as a function of angle of attack at Mach numbers of 0.5 and 0.92

for an aspect-ratio-4.0, unswept wing configuration (reference 13). The horizontal tail was mounted either in the plane of the wing extended or at a high position in which the tail height over tail length corresponded to an angle of 15°. As with the swept or delta configurations, the airplane with the horizontal tail in the low position had greater stability than the high-tail model in some moderate to high angle-of-attack range. In this case, however, the total stability changes with angle of attack are about equally large for the high- or low-tail models as contrasted to the swept or delta configurations on which the stability changes for the low tail were noticeably less than for the high tail.

The discussion up to this point has been concerned with the variation of stability with angle of attack. Of equal importance is the variation of stability with Mach number. Some static-longitudinal-stability and trim data for three widely different supersonic aircraft are examined. See references 14 to 23. The configurations considered are shown in figure 6. The first configuration has a swept wing and horizontal tail, the second a straight wing and tail, and the third is a tailless delta.

Also presented in figure 6 is the variation of the aerodynamic center in percent of the mean aerodynamic chord behind the leading edge of the mean aerodynamic chord. As is to be expected, the aerodynamic center moves back at supersonic speeds. It is interesting to note that the total aerodynamic-center travel, in feet, for all these aircraft is of the same order of magnitude, about 2.5 to 2.75 feet.

As a consequence of the increased stability, it is to be expected that the maneuverability of all these aircraft will be less at supersonic speeds than at subsonic speeds. Figure 7 presents the variation of trim lift coefficient with Mach number for several control deflections. Since complete trim data were not available, estimations were made in certain regions as indicated by the dotted lines. Also shown are estimated values of maximum lift. The control for the swept and unswept configuration is an all-movable tail whereas that for the delta configuration is a constant-chord trailing-edge elevon.

Note that all the configurations have adequate control to attain maximum lift at subsonic speeds, but that only the unswept-wing airplane has enough control effectiveness at supersonic speeds to attain maximum lift without inordinately large control deflections. In this connection it is necessary to point out, however, that the straight-wing configuration has a tail-volume coefficient $\frac{S_t}{S}\frac{l_t}{l}$ that is about 2.5 times that of the swept configuration. Another factor which must be considered is that the design wing loadings for these aircraft are quite different. The wing loading for the sweptback configuration is about 60, for the unswept configuration about 120, and for the tailless delta configuration

about 30. For a given altitude of flight and normal acceleration, therefore, the unswept-wing aircraft requires twice as much lift coefficient as the swept-wing aircraft and four times as much as the delta configuration.

Another significant consideration of static stability and trim is the control deflection as a function of Mach number for trim at a given value of acceleration. Figure 8 presents control deflection as a function of Mach number for trim at zero lift and for trim in level flight at 40,000 feet.

As can be noted from figure 7 there is a pitch-up tendency at low values of lift coefficient near a Mach number of 1.0 for all these aircraft. This result is evident in the control deflection required to trim at zero lift for the swept-wing configuration; for instance, more trailing-edge down movement of the all-movable tail is required as the Mach number range is traversed from subsonic to supersonic speeds. It is interesting to note that this same pitch-up has occurred in many rocket-propelled model tests of aircraft configurations (references 24 to 27). The only thing common to all these aircraft was the asymmetry usually associated with an airplane, for instance, vertical tail above the center of gravity, horizontal tail in a region in which there is downwash at zero lift due to flow around the tail of the fuselage.

An examination of the control required to trim in level flight indicates regions for all the aircraft in which more up-control is required to trim as the Mach number increases. This result has been noted in flight tests of supersonic research aircraft and so far pilots have not particularly objected since the aircraft is stable in the sense that more up-control, at a constant speed, gives increasing normal acceleration. This unstable variation of control with Mach number, however, is probably not a desirable characteristic if the airplane is to be flown in sustained level flight in this speed range. This unstable variation of control with Mach number indicates that a divergence in speed will occur if the airplane is disturbed from trim; therefore, for any particular design, calculations should be made to make sure that the divergence is slow enough to be controlled by the pilot.

In the case of the sweptback and unswept configuration, it is of interest to point out again the advantage of the all-moving tail as a means of control. This advantage is evident in figure 8 by the moderate changes in control required to trim over the Mach number range, as contrasted to the inordinately large amounts of elevator required by the Bell X-1.

Dynamic Stability

The following remarks on dynamic longitudinal stability are concerned with the characteristics of the short-period oscillation in pitch. Shown in figure 9 are some useful approximations for the period and damping characteristics of this oscillation. These expressions are the usual approximations, valid for two degrees of freedom and low damping. The various quantities have been arranged so that the effect of wing loading, scale, atmospheric properties, and aerodynamic properties may be seen by inspection. The quantities contained in these expressions are defined as follows:

Symbols:

C_m	pitching-moment coefficient
C_L	lift coefficient
P	period of the oscillation, seconds
$t_{1/10}$	time to damp to 1/10 amplitude, seconds
$C_{1/10}$	cycles to damp to 1/10 amplitude
k_y	radius of gyration in pitch, feet
$\bar{c}$	mean aerodynamic chord, feet
S	wing area, square feet
W	weight of airplane, pounds
M	Mach number
p	atmospheric static pressure, pounds per square foot
ρ	atmospheric density, slugs per cubic foot
V	velocity, feet per second
α	angle of attack, radians
θ	angle of pitch, radians
t	time, seconds

Subscripts:

$\dot{\alpha} = \frac{d\alpha}{dt}\frac{\bar{c}}{2V}$

$q = \frac{d\theta}{dt}\frac{\bar{c}}{2V}$

The symbols α, $\dot{\alpha}$, and q used as subscripts indicate the derivative of the quantity with respect to the subscript, for example $C_{m_\alpha} = \frac{dC_m}{d\alpha}$.

The quantity $C_{m_q} + C_{m_{\dot{\alpha}}}$ that appears in the expressions for damping gives the damping in pitch due to pitching velocity and rate of change of angle of attack with respect to time. On conventional aircraft, that is, aircraft having a wing and a horizontal tail mounted back of the wing, the horizontal tail always provides a predominate negative contribution to this derivative. Some of the airplanes that are being suggested for supersonic aircraft, however, are tailless-delta or swept-wing configurations. Since the theory indicates that these configurations might have very low negative or even positive values of $C_{m_q} + C_{m_{\dot{\alpha}}}$ in the transonic region, it is of interest to examine some available wind-tunnel and rocket-model measurements of this pitch-damping derivative for delta and sweptback wings.

The quantity $C_{m_q} + C_{m_{\dot{\alpha}}}$ as a function of Mach number is given in figure 10 for several tailless delta-wing configurations. The tunnel oscillation test data are for three delta wings of aspect ratio 2, 3, and 4 which correspond to leading-edge sweep of 63°, 53°, and 45°, respectively. Note that the 45° delta configuration (reference 28) indicates a very wide region, $M = 0.94$ to $M = 1.35$, of unstable or positive values of $C_{m_q} + C_{m_{\dot{\alpha}}}$. Within the limits of the test data there were no instabilities obtained for the delta wings of aspect ratio 2 and 3. The rocket-model test data substantiate the tunnel data in that the results available from the 45° delta configuration indicate a region of positive $C_{m_q} + C_{m_{\dot{\alpha}}}$ approximately the same as the tunnel data. The rocket-test data of the 60° delta wing show that the damping in pitch for this configuration was maintained throughout the region of the test results.

Some preliminary tunnel and rocket-model data on $C_{m_q} + C_{m_{\dot{\alpha}}}$ variation with Mach number for a swept wing of aspect ratio 3.0 are shown

in figure 11. The subsonic tunnel test results for the wing alone indicate positive values of $C_{m_q} + C_{m_{\dot{\alpha}}}$ above a Mach number of 0.93. These results are substantiated by recent rocket-model tests of a tailless configuration with this same wing and having the axis of pitch or center of gravity at the same position as the tunnel model. The rocket-model data indicate that the region of instability is very narrow, from about $M = 0.93$ to $M = 0.99$. Additional confirmation of these results is indicated by the supersonic tunnel tests of a configuration having a slightly different wing plan form and a more rearward axis of rotation.

As can be seen from figure 9, the aerodynamic contribution to the damping consists of two terms, C_{L_α} and $\frac{C_{m_q} + C_{m_{\dot{\alpha}}}}{2\left(\frac{k_Y}{\bar{c}}\right)^2}$.

Figure 12 illustrates the relative contributions of these terms for a straight wing and tail configuration and for two tailless delta wings, one with 60° leading-edge sweep and the other with 45° leading-edge sweep.

In the upper left-hand part of figure 12 is shown the variation of $C_{m_q} + C_{m_{\dot{\alpha}}}$ with Mach number for these three configurations. Note that the values of $C_{m_q} + C_{m_{\dot{\alpha}}}$ for the configuration with a horizontal tail are 5 to 10 times the magnitude of those for the tailless delta wings. When these values of $C_{m_q} + C_{m_{\dot{\alpha}}}$ are divided by the appropriate radius-of-gyration factor (upper right-hand part of fig. 12) note that the rotary damping factor of the tailless 60° delta wing and the airplane with tail are practically identical. This identity is fortuitous in this case; however, it does indicate one fallacy of comparing damping on the basis of $C_{m_q} + C_{m_{\dot{\alpha}}}$ alone. The lower left-hand part of figure 12 gives the variation of lift-curve slope C_{L_α} with Mach number. Note that, for the two configurations which maintained negative damping in pitch, the C_{L_α} contribution to the aerodynamic damping is of the same order of magnitude as the $\frac{C_{m_q} + C_{m_{\dot{\alpha}}}}{2\left(\frac{k_Y}{\bar{c}}\right)^2}$ contribution. This result again points to the necessity of considering two degrees of freedom for all dynamic longitudinal-stability calculations. Finally, the total aerodynamic-damping term as a function of Mach number indicates that all the configurations have aerodynamic damping of the same order of magnitude. The particular point of interest with regard to the

45° tailless delta wing is that, when the total aerodynamic damping in pitch is considered, the apparent region of instability as indicated by the $C_{m_q} + C_{m_{\dot{\alpha}}}$ term has been greatly reduced and might even be eliminated.

The period, time to damp to 1/10 amplitude, and cycles to damp to 1/10 amplitude have been calculated as a function of Mach number for the straight wing and tail configuration and for the 60° tailless delta wing. The results presented in figure 13 are for level flight at 40,000 feet, wing loading of 120 for the straight-wing airplane, and wing loading of 30 for the tailless delta wing. Note that, in general, the variations of P, $t_{1/10}$, and $C_{1/10}$ with Mach number are similar for both airplanes. The period decreases quite appreciably with increasing Mach number, but the time to damp to 1/10 amplitude is relatively constant; an increase in the cycles required to damp to 1/10 amplitude results. The present requirement for damping is $C_{1/10} = 1.0$ and is indicated by the shaded band. Note that neither configuration meets this requirement. The fact that the delta-wing configuration has the better damping in terms of $C_{1/10}$ might be expected since it has a much lower wing loading than the straight-wing airplane. See figure 9 which indicates that $C_{1/10} \sim \sqrt{W/S}$.

This poor damping in terms of $C_{1/10}$ may be objectionable from several viewpoints. In the first place it probably means that the aircraft will tend to have sustained small-amplitude oscillations in pitch due to random disturbances. Another possible objection is illustrated in figure 14. The characteristics of two oscillations in angle of attack following a step-function movement of the horizontal control are plotted as a function of time in the upper part of figure 14. The first oscillation is for a typical subsonic case in which the damping meets present requirements, that is, $C_{1/10} = 1.0$. The second oscillation is a supersonic case in which $C_{1/10} = 5.0$. The maximum overshoot $\Delta\alpha_m$ above the desired trim value is about 2.5 times as great for the $C_{1/10} = 5.0$ oscillation as for the $C_{1/10} = 1.0$ oscillation. For other values of damping this maximum overshoot may be estimated from the plot (also fig. 14) of maximum overshoot parameter $100 \frac{\Delta\alpha_m}{\alpha_t}$ as a function of cycles to damp to 1/10 amplitude $C_{1/10}$. This result indicates that an airplane having lightly damped pitch oscillations might inadvertently attain higher load factors in a sharp pull-up, for instance, than an airplane having a well-damped oscillation in pitch.

CONCLUDING REMARKS

On the basis of the information presented in this paper, the following conclusions are indicated.

For plain swept- and delta-wing aircraft configurations, a more nearly linear variation of pitching moment with angle of attack will probably be obtained with the horizontal tail mounted in a relatively low position.

The large increase in stability associated with flight from subsonic to supersonic speeds should not prevent the attainment of adequate maneuverability at supersonic speeds.

For tailless delta-wing aircraft configurations, those having the lower aspect ratio are more likely to have stable, that is, negative, values of the pitch damping factor $C_{m_q} + C_{m_{\dot{\alpha}}}$ throughout the Mach number range.

Low values of damping associated with the short-period longitudinal oscillation result in larger maximum loads in sharp pull-ups.

Langley Aeronautical Laboratory
National Advisory Committee for Aeronautics
Langley Field, Va.

REFERENCES

1. Allen, Edwin C.: Investigation of a Triangular Wing in Conjunction with a Fuselage and Horizontal Tail to Determine Downwash and Longitudinal-Stability Characteristics - Transonic Bump Method. NACA RM A51F12a, 1951.

2. Graham, David, and Koenig, David G.: Tests in the Ames 40- by 80-Foot Wind Tunnel of an Airplane Configuration with an Aspect Ratio 2 Triangular Wing and an All-Movable Horizontal Tail - Longitudinal Characteristics. NACA RM A51B21, 1951.

3. Jaquet, Byron M.: Effects of Horizontal-Tail Position, Area, and Aspect Ratio on Low-Speed Static Longitudinal Stability and Control Characteristics of a 60° Triangular-Wing Model Having Various Triangular-All-Movable Horizontal Tails. NACA RM L51I06, 1951.

4. Goodman, Alex: Effects of Wing Position and Horizontal-Tail Position on the Static Stability Characteristics of Models with Unswept and 45° Sweptback Surfaces with Some Reference to Mutual Interference. NACA TN 2504, 1951.

5. Foster, Gerald V., and Fitzpatrick, James E.: Longitudinal-Stability Investigation of High-Lift and Stall-Control Devices on a 52° Sweptback Wing with and without Fuselage and Horizontal Tail at a Reynolds Number of 6.8×10^6. NACA RM L8I08, 1948.

6. Foster, Gerald V., and Griner, Roland F.: Low-Speed Longitudinal and Wake Air-Flow Characteristics at a Reynolds Number of 5.5×10^6 of a Circular-Arc 52° Sweptback Wing with a Fuselage and a Horizontal Tail at Various Vertical Positions. NACA RM L51C30, 1951.

7. Osborne, Robert S.: A Transonic-Wing Investigation in the Langley 8-Foot High-Speed Tunnel at High Subsonic Mach Numbers and at a Mach Number of 1.2. Wing-Fuselage Configuration Having a Wing of 45° Sweepback, Aspect Ratio 4, Taper Ratio 0.6, and NACA 65A006 Airfoil Section. NACA RM L50H08, 1950.

8. Donlan, Charles J., Myers, Boyd C., II, and Mattson, Axel T.: A Comparison of the Aerodynamic Characteristics at Transonic Speeds of Four Wing-Fuselage Configurations as Determined from Different Test Techniques. NACA RM L50H02, 1950.

9. Purser, Paul E., Spearman, M. Leroy, and Bates, William R.: Preliminary Investigation at Low Speed of Downwash Characteristics of Small-Scale Sweptback Wings. NACA TN 1378, 1947.

10. Myers, Boyd C., II, and King, Thomas J., Jr.: Aerodynamic Characteristics of a Wing with Quarter-Chord Line Swept Back 45°, Aspect Ratio 4, Taper Ratio 0.3, and NACA 65A006 Airfoil Section. Transonic-Bump Method. NACA RM L9E25, 1949.

11. Myers, Boyd C., II, and King, Thomas J., Jr.: Aerodynamic Characteristics of a Wing with Quarter-Chord Line Swept Back 60°, Aspect Ratio 2, Taper Ratio 0.6, and NACA 65A006 Airfoil Section. Transonic-Bump Method. NACA RM L50A12, 1950.

12. King, Thomas J., Jr., and Myers, Boyd C., II: Aerodynamic Characteristics of a Wing with Quarter-Chord Line Swept Back 60°, Aspect Ratio 4, Taper Ratio 0.6, and NACA 65A006 Airfoil Section. NACA RM L9G27, 1949.

13. Johnson, Ben H., Jr., and Rollins, Francis W.: Investigation of a Thin Wing of Aspect Ratio 4 in the Ames 12-Foot Pressure Wind Tunnel. V - Static Longitudinal Stability and Control throughout the Subsonic Speed Range of a Semispan Model of a Supersonic Airplane. NACA RM A9I01, 1949.

14. Spearman, M. Leroy, and Robinson, Ross B.: The Aerodynamic Characteristics of a Supersonic Aircraft Configuration with a 40° Sweptback Wing through a Mach Number Range from 0 to 2.4 as Obtained from Various Sources. NACA RM L52A21, 1952.

15. D'Aiutolo, Charles T., and Mason, Homer P.: Preliminary Results of the Flight Investigation between Mach Numbers of 0.80 and 1.36 of a Rocket-Powered Model of a Supersonic Airplane Configuration Having a Tapered Wing with Circular-Arc Sections and 40° Sweepback. NACA RM L50H29a, 1950.

16. Weil, Joseph, Comisarow, Paul, and Goodson, Kenneth W.: Longitudinal Stability and Control Characteristics of an Airplane Model Having a 42.8° Sweptback Circular-Arc Wing with Aspect Ratio 4.00, Taper Ratio 0.50, and Sweptback Tail Surfaces. NACA RM L7G28, 1947.

17. Ellis, Macon C., Jr., Hasel, Lowell E., and Grigsby, Carl E.: Supersonic-Tunnel Tests of Two Supersonic Airplane Model Configurations. NACA RM L7J15, 1947.

18. Spearman, M. Leroy: An Investigation of a Supersonic Aircraft Configuration Having a Tapered Wing with Circular-Arc Sections and 40° Sweepback. Static Longitudinal Stability and Control Characteristics at a Mach Number of 1.40. NACA RM L9L08, 1950.

19. Spearman, M. Leroy, and Hilton, John H., Jr.: An Investigation of a Supersonic Aircraft Configuration Having a Tapered Wing with Circular-Arc Sections and 40° Sweepback. Static Longitudinal Stability and Control Characteristics at a Mach Number of 1.59. NACA RM L50E12, 1950.

20. Mitcham, Grady L., Crabill, Norman L., and Stevens, Joseph E.: Flight Determination of the Drag and Longitudinal Stability and Control Characteristics of a Rocket-Powered Model of a 60° Delta-Wing Airplane from Mach Numbers of 0.75 to 1.70. NACA RM L51I04, 1951.

21. Scherrer, Richard, and Wimbrow, William R.: Wind-Tunnel Investigation at a Mach Number of 1.53 of an Airplane with a Triangular Wing. NACA RM A7J05, 1948.

22. Lawrence, Leslie F., and Summers, James L.: Wind-Tunnel Investigation of a Tailless Triangular-Wing Fighter Aircraft at Mach Numbers from 0.5 to 1.5. NACA RM A9B16, 1949.

23. Gallagher, James J., and Mueller, James N.: Preliminary Tests to Determine the Maximum Lift of Wings at Supersonic Speeds. NACA RM L7J10, 1947.

24. Parks, James H., and Mitchell, Jesse L.: Longitudinal Trim and Drag Characteristics of Rocket-Propelled Models Representing Two Airplane Configurations. NACA RM L9L22, 1950.

25. Gillis, Clarence L., and Mitchell, Jesse L.: Flight Tests at Transonic and Supersonic Speeds of an Airplane-Like Configuration with Thin Straight Sharp-Edge Wings and Tail Surfaces. NACA RM L8K04a, 1949.

26. Vitale, A. James, McFall, John C., Jr., and Morrow, John D.: Longitudinal Stability and Drag Characteristics at Mach Numbers from 0.75 to 1.5 of an Airplane Configuration Having a 60° Swept Wing of Aspect Ratio 2.24 as Obtained from Rocket-Propelled Models. NACA RM L51K06, 1951.

27. Gillis, Clarence L., and Vitale, A. James: Wing-On and Wing-Off Longitudinal Characteristics of an Airplane Configuration Having a Thin Unswept Tapered Wing of Aspect Ratio 3, as Obtained from Rocket-Propelled Models at Mach Numbers from 0.8 to 1.4. NACA RM L50K16, 1951.

28. Tobak, Murray, Reese, David E., Jr., and Beam, Benjamin H.: Experimental Damping in Pitch of 45° Triangular Wings. NACA RM A50J26, 1950.

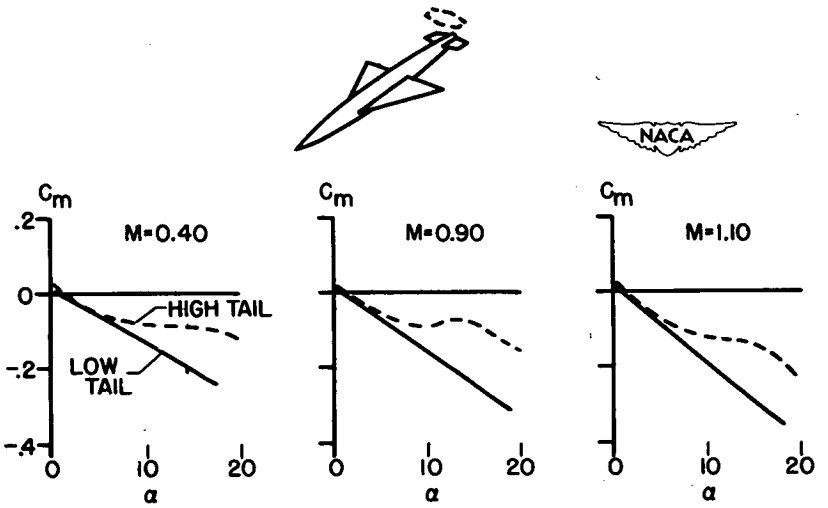

Figure 1.- Effect of tail height on the stability of a delta-wing aircraft.

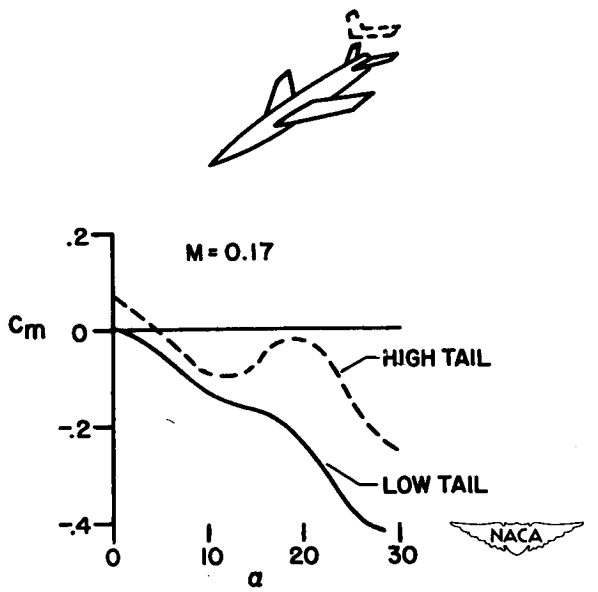

Figure 2.- Effect of tail height on the stability of a sweptback-wing aircraft.

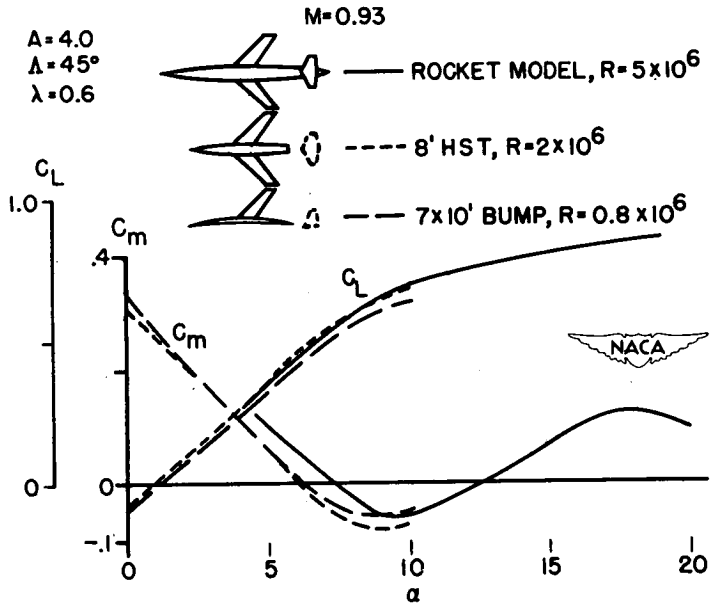

Figure 3.- Variation of lift and moment coefficient with angle of attack for a sweptback-wing aircraft having a horizontal tail located 0.50 semispan above the plane of the wing.

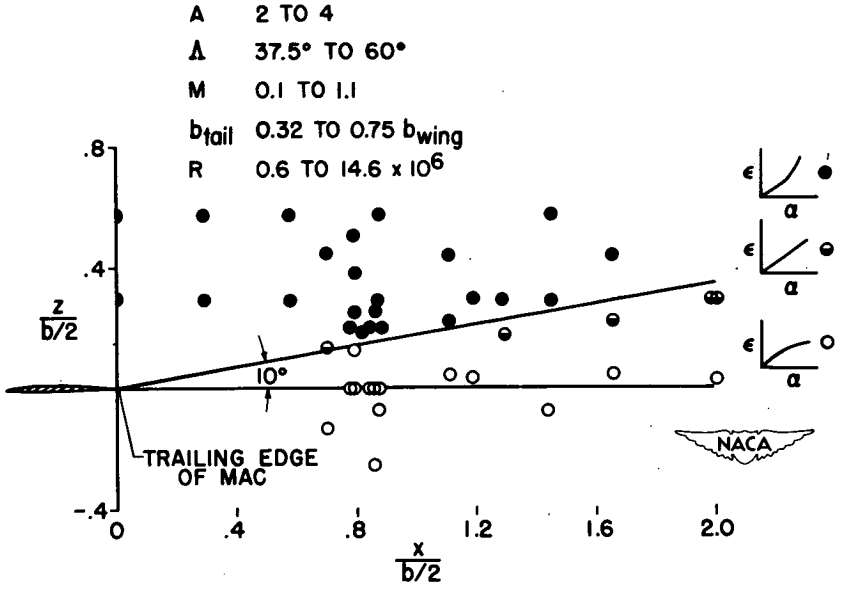

Figure 4.- Characteristics of the average downwash at horizontal-tail locations behind low-aspect-ratio swept and delta wings.

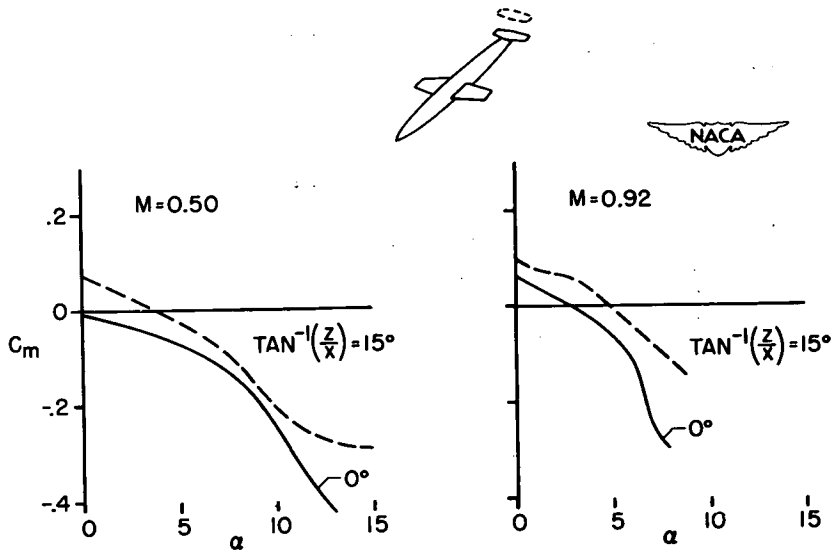

Figure 5.- Effect of tail height on the stability of an unswept-wing aircraft.

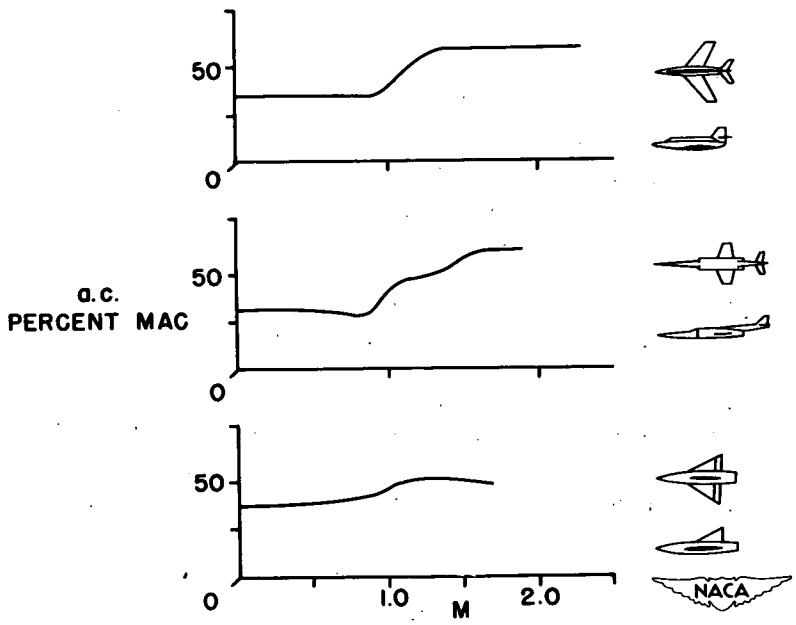

Figure 6.- Variation of aerodynamic center with Mach number for three supersonic aircraft.

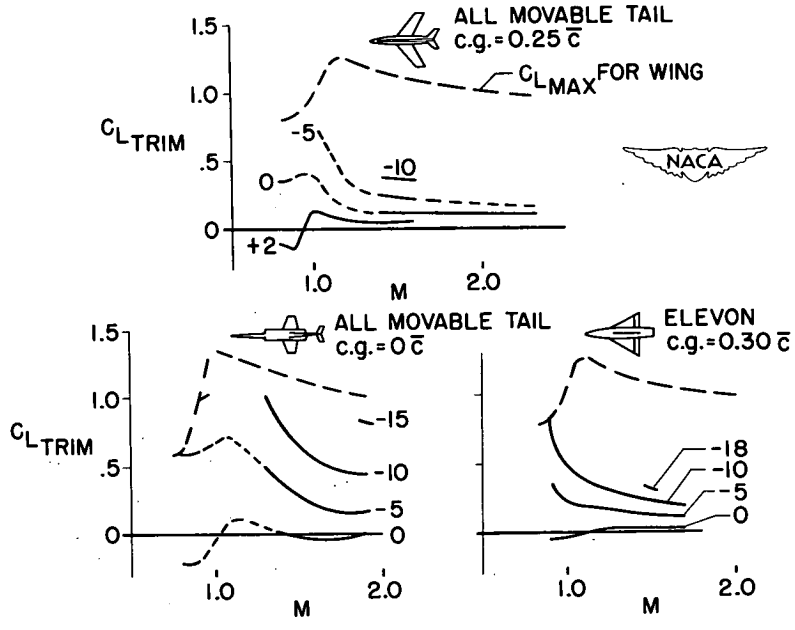

Figure 7.- Variation of trim lift coefficient with Mach number and with control deflection.

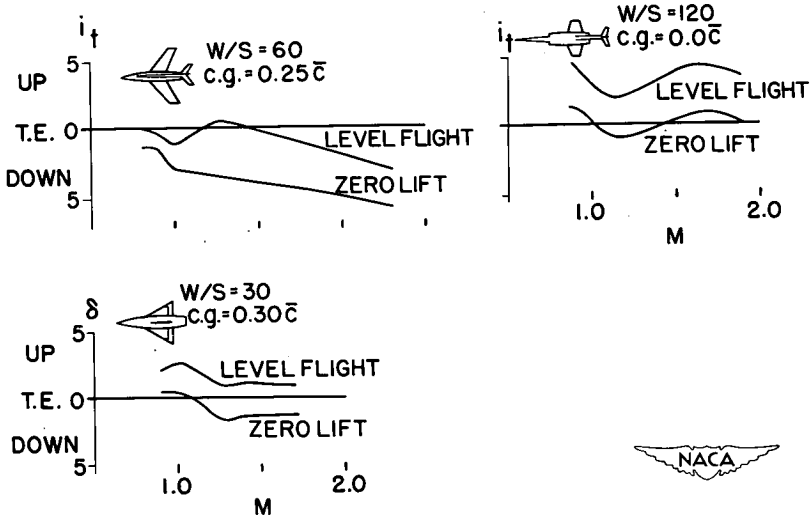

Figure 8.- Variation of control deflection with Mach number for trim at zero lift and for trim in level flight at 40,000 feet.

PERIOD, SECONDS

$$P \approx \frac{1.32\left(\frac{k_y}{\bar{c}}\right)\sqrt{\frac{W}{S}}\sqrt{\bar{c}}}{M\sqrt{\rho}\sqrt{-C_{m_\alpha}}}$$

TIME TO DAMP TO 1/10 AMPLITUDE, SECONDS

$$\frac{t_1}{10} \approx \frac{0.242\frac{W}{S}}{M\sqrt{\rho\rho}\left[C_{L_\alpha} - \frac{(C_{m_q} + C_{m_{\dot{\alpha}}})}{2\left(\frac{k_y}{\bar{c}}\right)^2}\right]}$$

CYCLES TO DAMP TO 1/10 AMPLITUDE

$$\frac{c_1}{10} = \frac{\frac{t_1}{10}}{P} \approx \frac{0.183\sqrt{\frac{W}{S}}\sqrt{-C_{m_\alpha}}}{\left(\frac{k_y}{\bar{c}}\right)\sqrt{\bar{c}}\sqrt{\rho}\left[C_{L_\alpha} - \frac{(C_{m_q} + C_{m_{\dot{\alpha}}})}{2\left(\frac{k_y}{\bar{c}}\right)^2}\right]}$$

NACA

Figure 9.- Some approximations for calculating the characteristics of the short-period longitudinal oscillation in pitch.

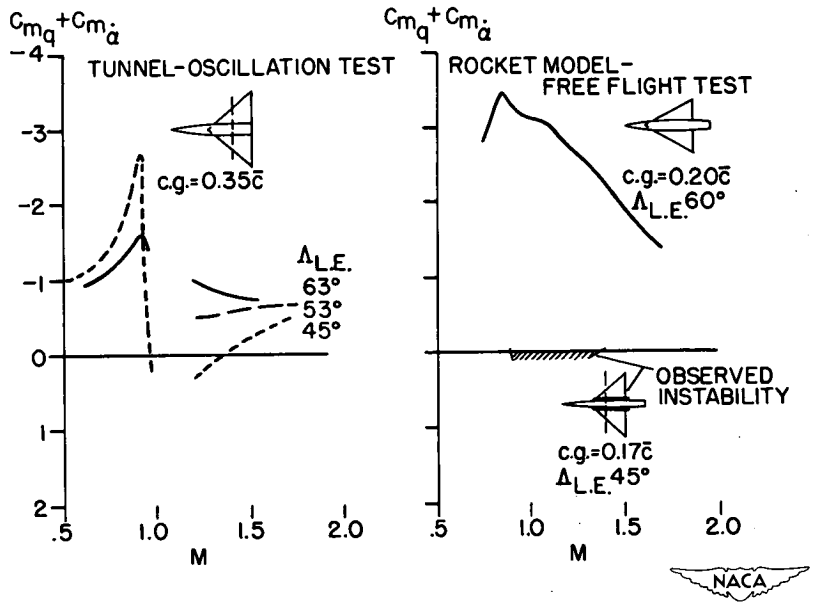

Figure 10.- Variation of the pitch-damping factor $C_{m_q} + C_{m_{\dot{\alpha}}}$ with Mach number for tailless delta-wing aircraft.

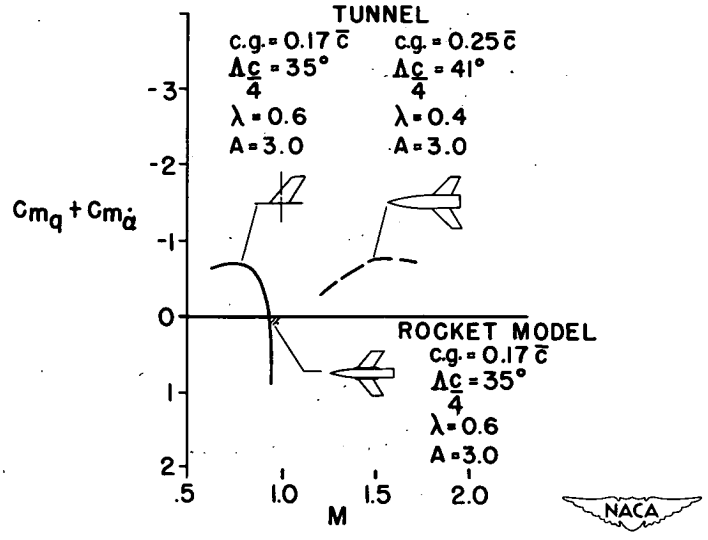

Figure 11.- Variation of the pitch-damping factor $C_{m_q} + C_{m_{\dot{\alpha}}}$ with Mach number for tailless sweptback-wing aircraft.

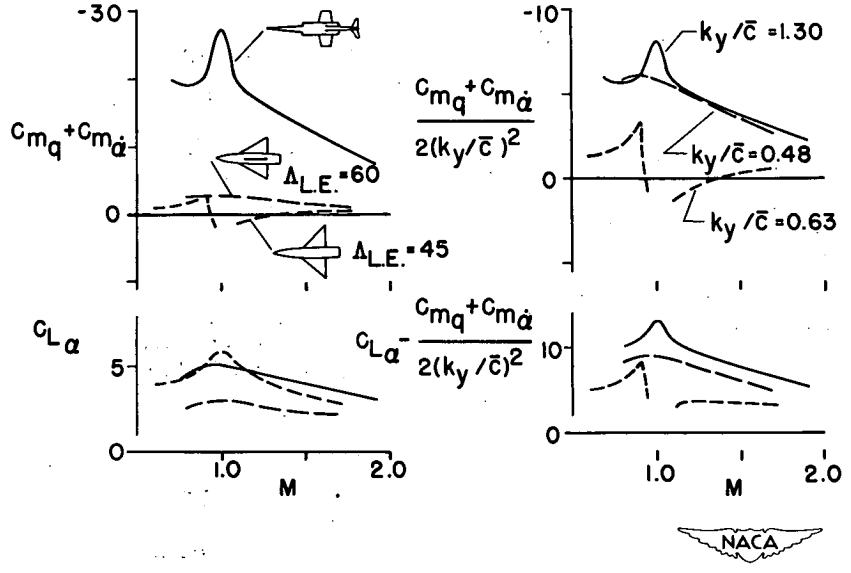

Figure 12.- A comparison of the damping-in-pitch factors for three supersonic aircraft configurations.

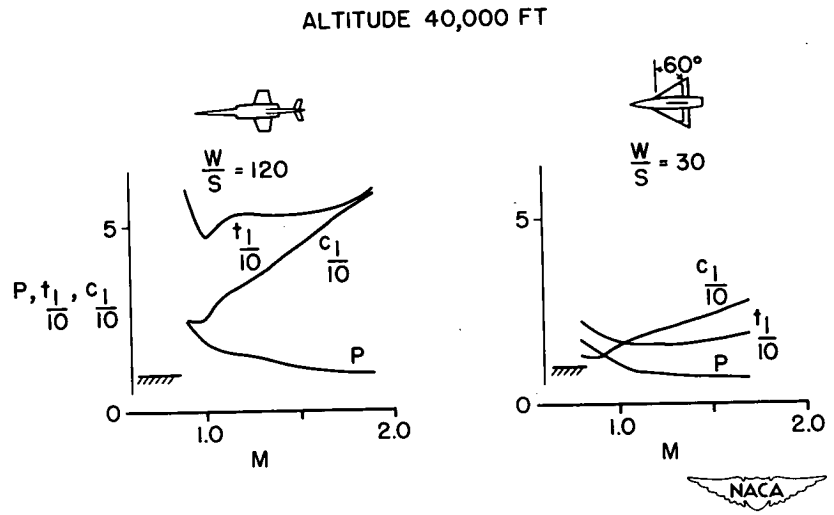

Figure 13.- Characteristics of the short-period longitudinal oscillation in pitch for two supersonic aircraft configurations.

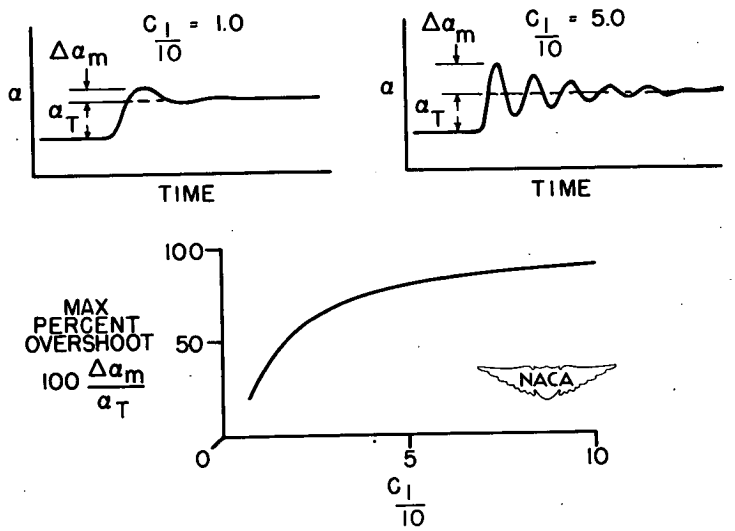

Figure 14.- Effect of damping on the maximum angle of attack attained after a step-function disturbance of the horizontal control.